Measurement of the grain-boundary states in semiconductors by deep-level transient spectroscopy

A. Broniatowski
Groupe de Physique des Solides de l'Ecole Normale Supérieure, Université de Paris VII, Tour 23, 2 place Jussieu, 75251 Paris Cédex 05, France
(Received 12 December 1986)

The paper deals with standing issues regarding the application of deep-level transient spectroscopy (DLTS) to the measurement of the electron states at grain boundaries in semiconductors: (i) The relationship between the density of interface states and the associated DLTS spectra is worked out quantitatively for the case in which the levels form a continuous distribution in energy, leading to simple analytical expressions for the emission rate, the density of states, and the capture cross section at the quasi-Fermi level of the trapped carriers. This treatment will also apply, with minor modifications, to different physical systems where interface states are present, e.g., the oxide-semiconductor interfaces. The effect of field-enhanced emission on the DLTS spectra of the boundary states is also considered. (ii) As a practical illustration, the grain-boundary parameters are determined for the $\Sigma=25$ twin boundary in n- and p-type doped silicon bicrystals. In n-type silicon, a single boundary level is found at $E_c-0.66$ eV, with a density of 2.6×10^{11} cm^{-2}. In p-type silicon, the boundary levels are continuously distributed in energy, with a density on the order of 10^{12} eV^{-1} cm^{-2} in the energy range ($E_v+0.2$ eV, $E_v+0.6$ eV). The density of states shows a sharp maximum at $E_v+0.18$ eV, associated with a single trap level, the density of which is on the order of 2×10^{11} cm^{-2}. The capture cross sections of the traps are on the order of 10^{-14} to a few 10^{-13} cm^2. These results are consistent with the data obtained from complementary capacitance-voltage and thermally-stimulated-capacitance experiments. The densities of states appear to be highly dependent on the thermal history of the specimens. Microanalytical investigations are currently in progress, aimed at clarifying the dependence of the electronic properties on impurity segregation at the grain boundaries in silicon.

I. INTRODUCTION

A number of studies have been devoted in the past years to the nature and properties of the grain-boundary levels in semiconductors, both from the experimental[1] and the theoretical[2] points of view. In particular, progress has been made towards the quantitative evaluation of the density of the boundary levels, taking advantage of well-established techniques for characterizing the defect states in semiconductors: admittance spectroscopy[3,4] and deep-level transient spectroscopy (DLTS).[5,6] Both techniques are based on a measurement of the carrier emission rate at the interface levels, either from the frequency response of the trap occupancy to an ac-modulated signal (admittance spectroscopy) or from the transient response to voltage pulses (DLTS). The purpose of this paper is to present new developments in the field of transient capacitance measurements with selected examples of application.

We shall first recall in Sec. II the principle of the application of the DLTS technique to single boundaries in bicrystalline samples.[7,8] We consider next the quantitative relationship between the spectra and the density of boundary states, with an emphasis on the case where the levels form a continuous distribution in energy (Sec. III). A formal treatment will be given of the corresponding nonexponential emission transients, leading to simple analytical relations between the DLTS spectrum and the density of interface states. For commodity reasons, only the basic relationships are given in the text; the detailed derivation of the formulas is postponed to an appendix. Capture cross-section measurements are then described, based on coupled transient capacitance and direct current measurements. Section III concludes with a discussion of electric field effects on carrier emission from the grain-boundary states, as reflected in the shape of the DLTS spectra. As a practical illustration, we shall evaluate in Sec. IV the grain-boundary parameters (density of states and capture cross section as a function of energy) in the case of the $\Sigma=25$ twin boundary in n- and p-type silicon bicrystals. A more complete discussion of the data obtained for this particular boundary and their dependence on annealing treatments will be found in Ref. 9.

II. THE APPLICATION OF DEEP-LEVEL TRANSIENT SPECTROSCOPY TO THE MEASUREMENT OF THE GRAIN-BOUNDARY STATES

We shall consider the case of a grain boundary in an n-type bicrystal; a similar description applying to the case of p-type material.

A. Obtaining DLTS spectra on single boundaries

The basic DLTS experiment consists of applying periodic voltage pulses across the boundary in order to vary the occupancy of the interface levels (Fig. 1). Between successive pulses, the boundary charge relaxes towards equilibrium by thermal emission of the excess trapped carriers, the emission rate from any level (E) in the density of states being given by

$$e_n=(\sigma/g)N_c v_{\rm th}\exp[(E-E_c)/kT]\ , \tag{1}$$

where σ represents the capture cross section and g the degeneracy of the trap, $v_{\rm th}$ the mean thermal velocity of the carriers, and N_c the effective number of states at the bottom of the conduction band (E_c).

Equation (1) is obtained by an application of the detailed-balance principle, and is therefore valid in principle at thermodynamic equilibrium only. Cases could be found where the capture and emission properties of the boundary traps are affected by the electric field at the interface. In such cases, the emission rates measured by DLTS will be different from those at thermodynamic equilibrium. Means to detect an effect of the electric field on carrier emission will be considered in Sec. III E in relation to the bias dependence of the grain-boundary spectra.

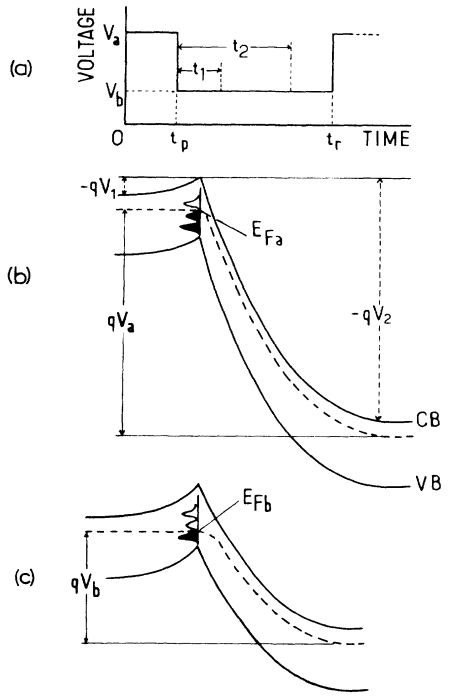

FIG. 1. (a) The pulse sequence for DLTS measurements of the grain-boundary levels. V_a, filling pulse amplitude; V_b, bias voltage; t_p, pulse duration; t_r, pulse repetition time; t_1,t_2, gate settings. (b) and (c) Bending of the energy bands under voltage V_a and V_b, showing the corresponding quasi-Fermi-levels E_{Fa} and E_{Fb}. CB, conduction band; VB, valence band. V_1 and V_2 represent the barrier heights on the negatively and the positively biased sides of the boundary, respectively.

The DLTS signal S is formed from the charge transient by means of a dual-gate correlator (boxcar averager or two-phase lock-in amplifier):

$$S(t_1,t_2)=Q(t_1)-Q(t_2)\ , \tag{2}$$

where $Q(t)$ represents the specific boundary charge at times t_1 and t_2, which are the gate settings of the correlator. By recording the variation of S as a function of the sample temperature, a spectrum characteristic of the boundary levels is obtained.

In practice, the quantity measured is not directly the boundary charge but rather the related geometric (high-frequency) capacitance:

$$C=q\epsilon N_d/|Q|\ , \tag{3}$$

where q represents the elementary positive charge, ϵ the dielectric constant of the material, and N_d the doping level in the depleted region on both sides of the interface. Thus the DLTS signal must be formed from the reciprocal, rather than from the direct value of the sample capacitance. This can be achieved either by digital or by analog processing of the capacitance transients. In our case, an analog system was used, the capacitance signal being inverted by means of a wide-band multiplier or divider amplifier before processing through the correlator. With the proper calibration, the DLTS signal is thus directly obtained in units of charge per unit boundary area.

B. The bias dependence of the grain-boundary spectrum

DLTS spectra depend for their characteristics on the amplitude (V_a) and the width of the filling pulses, as well as the offset voltage V_b [Fig. 1(a)]. For simplicity, we shall limit ourselves to the case where the filling pulses are long enough that a quasisteady state is reached at the end of the pulse. In the steady state, the occupancy of the boundary levels is conveniently described using the notion of a quasi-Fermi-level (QFL) of the trapped carriers.[10] Denoting by E_{Fa} and E_{Fb} the QFL's corresponding to the voltages V_a and V_b, respectively [Figs. 1(b) and (c)], we then obtain a spectrum of the boundary levels in the energy range (E_{Fa},E_{Fb}). By varying V_a and V_b, the energy window can be adjusted to visualize selected parts of the density of states. An example of this is given by Fig. 2, where a set of spectra is presented for the case of the $\Sigma=25$ boundary in a p-type silicon bicrystal. The spectrum (1) ($V_a=8$ V, $V_b=0$ V) just forms the envelope of the spectra (2) ($V_a=4$ V, $V_b=0$ V) and (3) ($V_a=8$ V, $V_b=4$ V), in accordance with the respective locations of the QFL's for the three different values of the applied voltage (0, 4 and 8 V). In this procedure we are limited, however, by the voltage dependence of the trap occupancy. On the one hand, only those states empty at equilibrium can be measured in a DLTS experiment. On the other hand, traps close to the conduction-band edge can only be detected using large-amplitude filling pulses. A case will be discussed in Sec. IV, where pulses up to 100 V must be applied in order to detect the shallower part of the density

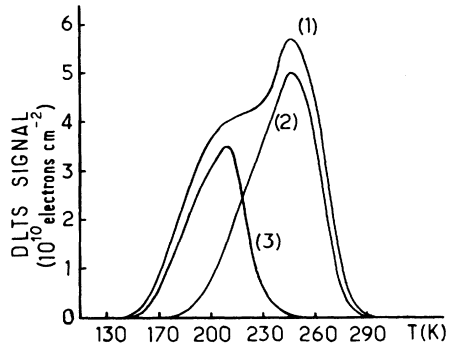

FIG. 2. DLTS spectra of the $\Sigma=25$ boundary levels in a p-type silicon bicrystal, boron doped to 8.0×10^{14} cm^{-3}. Sample annealed for 24 h at 750 °C under nitrogen flow. Spectrum (1): $V_a=8$ V, $V_b=0$ V. Spectrum (2): $V_a=4$ V, $V_b=0$ V. Spectrum (3): $V_a=8$ V , $V_b=4$ V. Emission rate, 20 s^{-1}; pulse duration, 30 ms.

of states.

Let us consider next the features of the DLTS spectra for different forms of the density of states, starting with the simple case where the boundary levels form a discrete distribution in energy.

C. The spectrum obtained for discrete energy levels

In such cases, the spectrum consists of a succession of peaks, each of them associated with a particular boundary level. Figure 3(a) represents, for example, the spectrum obtained for the $\Sigma=25$ boundary in an n-type silicon bicrystal:[11] the spectrum reduces to one peak associated with a single boundary level. The emission transient then has the shape of a simple exponential: $\Delta Q(t)=qN_t\exp(-e_nt)$ where N_t represents the trap density. As a result, it is shown that the maximum of the DLTS signal occurs at the temperature T where the carrier emission rate has the value[6]

$$e_n=(t_2-t_1)^{-1}\ln(t_2/t_1)\ . \tag{4}$$

The dependence of e_n on T is obtained from a series of spectra for different gate settings (t_1,t_2). The activation energy for carrier emission is then deduced from an Arrhenius plot of $\ln(e_n)$ versus $1/T$ (the signature of the trap). For a determination of N_t, large-amplitude filling pulses must be used to ensure that all states are counted. N_t is then deduced from the peak amplitude of the signal S_m using the relationship

$$S_m=qN_t[(1/r)^{1/(r-1)}-(1/r)^{r/(r-1)}]\ , \tag{5}$$

where $r=t_2/t_1$. In the case presented, the signature of the trap [Fig. 3(b)] gives an energy level at $E_c-0.66$ eV with the density $N_t=2.6\times10^{11}$ cm^{-2}.

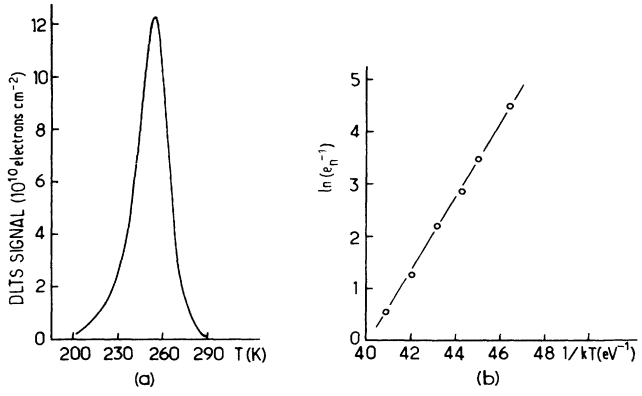

FIG. 3. (a) Spectrum obtained for the $\Sigma=25$ boundary in an n-type silicon bicrystal, phosphorus doped to 3.6×10^{14} cm^{-3}. Sample annealed for 2 h at 900 °C under argon + water vapor. $V_a=20$ V, $V_b=0$ V; emission rate, 28 s^{-1}; pulse duration, 20 ms. (b) Signature of the trap, giving an energy level at $E_c-0.66$ eV.

III. THE SPECTRUM ASSOCIATED WITH A CONTINUUM OF BOUNDARY STATES

More frequently, the spectrum shows a smooth modulation with temperature [Fig. 7(a)]. Similar features have been observed in different systems, notably in the case of the traps at oxide-semiconductor interfaces.[12] Such spectra depend for their evaluation on an analysis of the nonexponential emission transients associated with a continuum of interface states. We shall examine successively the determination of the grain-boundary parameters (carrier emission rate, density of states, and capture cross section) at the quasi-Fermi level E_{Fa} under voltage V_a.

A. Measurement of the carrier emission rate at the quasi-Fermi-level E_{Fa}

Let $N(E)$ represent the density of the boundary states as a function of energy E [Fig. 4(a)]. The boundary charge at the end of the filling pulse (which we take as $t=0$) is given by

$$Q(0)=q\int_{E_v}^{E_c}N(E)f(E-E_{Fa})dE\ , \tag{6}$$

where $f(E-E_{Fa})$ represents the quasi-Fermi distribution under voltage V_a:

$$f(E-E_{Fa})=\{1+[1/g(E)]\exp[(E-E_{Fa})/kT]\}^{-1}\ , \tag{7}$$

including the factor $g(E)$ to account for the effect of trap degeneracy on the occupation statistics. At $t=0$ the voltage is reduced to the value V_b with the corresponding QFL E_{Fb}. The boundary charge then relaxes to the new value

$$Q(\infty)=q\int_{E_v}^{E_c}N(E)f(E-E_{Fb})dE\ . \tag{8}$$

The relaxation of the charge may involve, in addition to the direct emission of electrons into the conduction band, a more complex redistribution of the carriers among vacant boundary states. We shall assume for simplicity that such transitions can be neglected, so that the various traps relax independently. Then, the occu-

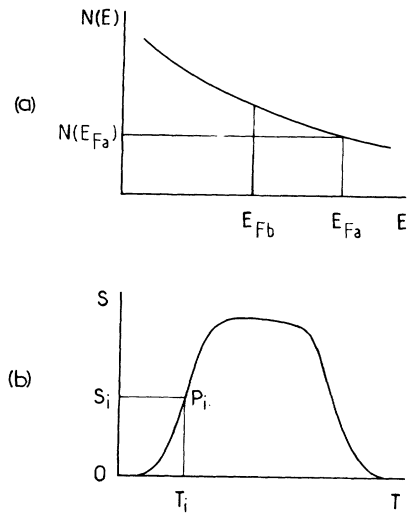

FIG. 4. (a) The density of states $N(E)$ as a function of energy E, showing the respective QFL's E_{Fa} and E_{Fb} under voltages V_a and V_b, and the density of states $N(E_{Fa})$. (b) The corresponding DLTS spectrum for some values (t_1,t_2) of the gate settings. S, DLTS signal; T, temperature; P_i, inflection point on the low-temperature edge of the spectrum with the coordinates (T_i,S_i).

pancy of every single level obeys a simple law in $\exp(-e_n t)$ where e_n is given by Eq. (1). As a result, the charge transient $\Delta Q(t)=Q(t)-Q(\infty)$ is given by

$$\Delta Q(t)=q\int_{E_v}^{E_c} N(E)[f(E-E_{Fa})-f(E-E_{Fb})] \times \exp(-e_n t)dE \ . \tag{9}$$

Although the occupancy of every single level has an exponential decay with time, the net charge transient is clearly nonexponential. Let us examine in more detail the variation of the trap occupancy as a function of time. Due to the sharp dependence of the emission rates on energy, the initial part of the transient is associated with carrier emission from levels close to E_{Fa}. At later times deeper states will be involved until finally a steady state is reached with QFL E_{Fb}. These properties are reflected in the temperature dependence of the DLTS signal [Fig. 4(b)]: at low temperatures the signal is zero due to the freezing of carriers at all the boundary levels. The initial rise of the signal is associated with emission from the traps in the vicinity of E_{Fa}. As the temperature increases, deeper states come into play until finally the signal returns to zero as the emission rate for all states in the range (E_{Fa},E_{Fb}) becomes larger than t_1^{-1}. At this point, we note that Eq. (9) takes no account of the trapping of carriers at the boundary levels. For the conditions prevailing in DLTS experiments, carrier trapping is important only in the final part of the transient, where the boundary charge reaches its steady-state value under voltage V_b. Accordingly, we shall exclude from our discussion the final drop of the DLTS signal at high temperatures, where the emission rate at the quasi-Fermi-level E_{Fb} becomes comparable with t_1^{-1}.

The formal analysis of the spectrum focuses on the evaluation of the emission rate $e_n(E_{Fa})$. For this purpose, let us consider the low-temperature branch of the spectrum [Fig. 4(b)]: along that branch an inflection point P_i is met with the coordinates (T_i,S_i). It is then shown (Appendix, Secs. 1 and 2) that for $T=T_i$, $e_n(E_{Fa})$ has a value uniquely determined by the gate settings of the correlator. To express this relationship, let us define the parameters

$$r=t_2/t_1 \tag{10}$$

and

$$u=g(E_{Fa})t_1 e_n(E_{Fa}) \ , \tag{11}$$

where $g(E_{Fa})$ represents the degeneracy of the level E_{Fa}. u is then determined as a function of r by the implicit equation

$$r=h(u)/h(ru) \ , \tag{12}$$

where

$$h(x)=(1+x)e^x \mathbb{E}_1(x)-1 \ , \tag{13}$$

and

$$\mathbb{E}_1(x)=\int_x^\infty t^{-1}e^{-t}dt \tag{14}$$

defines Euler's function of the first order.[13] Figure 5 represents (solid curve) the variation of $[g(E_{Fa})t_1 e_n(E_{Fa})]^{-1}$ as a function of t_2/t_1 as deduced from these equations. For comparison, the variation of $(t_1 e_n)^{-1}$ for a single level [Eq. (4)] is also represented (dotted line). Due to the difference in the form of the emission transients, the dependence of e_n on t_1 and t_2 is somewhat different for a continuum of states and a single level. However, the procedure to obtain the signature of the traps is quite similar in both cases: starting from a set of spectra for different gate settings, the product $g(E_{Fa})e_n(E_{Fa})$ is measured as a function of T_i and the activation energy for carrier emission is then deduced from an Arrhenius plot of $\ln[g(E_{Fa})e_n(E_{Fa})]$ versus $1/T_i$.

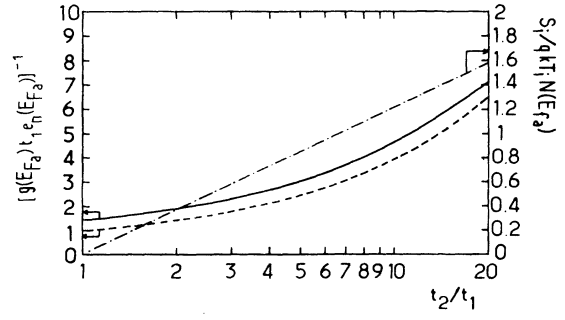

FIG. 5. Solid line: plot of $[g(E_{Fa})t_1 e_n(E_{Fa})]^{-1}$ vs t_2/t_1 as given by Eqs. (10)–(14). For comparison, the variation of $(t_1 e_n)^{-1}$ for a single trap level [Eq. (4)] is also represented, by the dotted line. Dot-dashed line: variation of $S_i/qkT_iN(E_{Fa})$ vs t_2/t_1 as given by Eq. (15).

It will be noted that the quantity effectively measured at T_i is not simply $e_n(E_{Fa})$, but rather the product $g(E_{Fa})e_n(E_{Fa})$. As far as the determination of the activation energies is concerned, this makes little difference as the emission rate is just multiplied by a constant (not temperature-dependent) factor. A more basic question arises when we consider the reason emission rate measurements should involve the g factor in the case of a continuum of states, although it does not appear in the case of a discrete level [Eq. (4)]. As discussed in the Appendix, Sec. 3, the reason rests with the fact that the emission rate measured at T_i is actually a weighted average of the rates of emission of the various traps within the width ΔE of the quasi-Fermi-distribution $f(E-E_{Fa})$. It then follows from the detailed calculation of the DLTS signal (Secs. 1 and 2 of the Appendix) that the average rate [whose value in terms of t_1 and t_2 is given by the set of equations (10)–(14)] is precisely $g(E_{Fa})e_n(E_{Fa})$. Equation (1) shows that this is just the emission rate expected for a level located at the center of the distribution: $E_1=E_{Fa}+kT_i \lng(E_{Fa})$.

B. The density of states at the level E_{Fa}

The relationship between the signal amplitude S_i at the inflection point of the spectrum and the density of states $N(E_{Fa})$ is derived in Sec. 1 of the Appendix as follows:

$$S_i=qkT_iN(E_{Fa})[\ln r+e^{ru}\mathbb{E}_1(ru)-e^{u}\mathbb{E}_1(u)] , \quad (15)$$

where r and u are defined by Eqs. (10) and (11). As mentioned before, the DLTS signal at T_i involves the states of energy within the width of the quasi-Fermi-distribution $f(E-E_{Fa})$. As a result, $N(E_{Fa})$ as given by Eq. (15) represents in fact an average of the density of states over that range of energies. The proportionality factor $[\ln r+e^{ru}\mathbb{E}_1(ru)-e^{u}\mathbb{E}_1(u)]$ is represented as a function of r by the dot-dashed line in Fig. 5.

C. The capture cross section $\sigma(E_{Fa})$

Capture cross-section measurements involve the dual determination of the carrier flux through the grain-boundary plane, and the rate of carrier trapping at the interface states. We shall show that, providing the emission rate from the boundary levels is not dependent on the electric field at the interface, a simple procedure applies to measure the capture cross section $\sigma(E_{Fa})$. Let us then start with the boundary in the steady state under voltage V_a, and denote by $\phi(V_a)$ the sum of the electron fluxes impinging from both grains on the boundary plane [Fig. 1(b)]. The probability per unit time of an electron being captured by the trap of energy E is given by $(1-f)\sigma(E)\phi(V_a)$, where $\sigma(E)$ represents the capture cross section and f the occupancy of the trap. On the other hand the emission probability is $e_n(E)f$. In the steady state both probabilities equalize, so that $(1-f)\sigma(E)\phi(V_a)=e_n(E)f$. Consider in particular the case of the QFL E_{Fa}. According to Eq. (7), the occupancy of that level is $f=g(E_{Fa})/[g(E_{Fa})+1]$ and therefore

$$\sigma(E_{Fa})=g(E_{Fa})e_n(E_{Fa})/\phi(V_a) . \quad (16)$$

We shall now express $\phi(V_a)$ as a function of the current density through the boundary. For this purpose, let us apply the thermoelectronic emission model of conduction over a potential barrier. Thus

$$\phi(V_a)=N_d v_{\rm th}[\exp(qV_1/kT)+\exp(qV_2/kT)] , \quad (17)$$

where N_d represents the free-carrier density in the bulk (identified for simplicity with the doping level of the material), and V_1 and V_2 are the barrier heights on the left- and right-hand sides of the boundary, respectively ($V_a=V_1-V_2$). On the other hand, the current density through the interface is given by

$$j(V_a)=qN_d v_{\rm th}[\exp(qV_2/kT)-\exp(qV_1/kT)] . \quad (18)$$

Combining Eqs. (16)–(18), we find for $\sigma(E_{Fa})$ the expression

$$\sigma(E_{Fa})=[qg(E_{Fa})e_n(E_{Fa})/j(V_a)]\tanh(qV_a/2kT) . \quad (19)$$

[A similar relationship is given in Eq. (12) of Ref. 10, for the case of a single trap level and assuming g equal to unity.]

A practical method follows to obtain the capture cross section $\sigma(E_{Fa})$, based on coupled transient capacitance and dc current measurements. Let us measure $g(E_{Fa})e_n(E_{Fa})$ at the temperature T_i, using the DLTS spectrum of the grain boundary for an appropriate choice of the filling-pulse amplitude (V_a), bias voltage (V_b), and gate settings (t_1,t_2). Let us also determine the current density $j(V_a)$ from the current-voltage characteristics of the boundary at the same temperature. Using these data, we then obtain $\sigma(E_{Fa})$ directly by means of Eq. (19).

The procedure just described clearly assumes the level E_{Fa} has the same emission rate for two different voltages V_a and V_b [at which $j(V_a)$ and $g(E_{Fa})e_n(E_{Fa})$ are measured, respectively]—a condition only fulfilled providing e_n is not affected by the electric field at the interface. We shall consider in Sec. III E the means to detect electric field effects on carrier emission. In cases where the emission rate happens to be field dependent, the quantity $g(E_{Fa})e_n(E_{Fa})$ will take different values depending on the applied voltage (V_b). Capture cross-section determinations then require more elaborate measurements than considered above, based on a detailed investigation of the kinetics of carrier trapping at the grain-boundary levels.[14–16] To the author's knowledge, this problem still remains to be solved for the case of a continuum of states.

To summarize, a procedure has been developed to obtain the emission rate, the density of states, and the capture cross section at the quasi-Fermi level of the trapped carriers. For a full description of the density of states these measurements should be repeated point after point for increasing values of the filling-pulse amplitude. We shall consider next a simplified, though possibly less accurate, method to obtain the density of states, starting from a single boundary spectrum.

D. A simplified procedure

As pointed out in Sec. II B, the DLTS spectrum is basically a representation of the density of states in the energy range (E_{Fa},E_{Fb}). Let us then apply large-amplitude filling pulses so that E_{Fa} is shifted upwards in the density of states, the aim being to involve in the spectrum the largest possible fraction of the boundary levels. The relationship between such spectra and the parent density of states has been worked out by several authors on the specific assumption that the capture cross section is a slowly varying function of energy.[12,17] It is then shown that the DLTS spectrum is related to the density of states by a simple axis transformation: the energy axis (E) being changed for the temperature axis (T) and the density-of-states axis $N(E)$ for that of the DLTS signal $S(T)$. The energy-temperature relationship is given by

$$E_c-E=kT\ln[(\sigma/g)N_c v_{\rm th}(t_2-t_1)/\ln(t_2/t_1)] \quad (20)$$

and the DLTS signal is related to the average density of states $N(E)$ in an energy range of width of approximately a few kT about $E(T)$, as follows:

$$S(T)=qN(E)kT\ln(t_2/t_1)\ . \quad (21)$$

Consider the energy-temperature correspondence as given by Eq. (20): while the dependence of E on temperature is approximately linear, that on σ is logarithmic only, and therefore much weaker. Thus, providing the various traps have comparable capture cross sections, the energy will be uniquely determined as a function of temperature. On the other hand, the energy scale could be strongly distorted in case σ has large variations with energy. For an order-of-magnitude estimate, let us suppose two different trap levels with the respective energies E_1 and E_2 and capture cross sections σ_1 and σ_2. According to Eq. (20), the condition that both traps should show up at the same temperature T_0 is given by

$$\sigma_2/\sigma_1\sim\exp[(E_1-E_2)/kT_0]\ . \quad (22)$$

For a numerical estimate, let us take $E_1-E_2=0.1$ eV and $T_0=116$ K: Eq. (22) then gives $\sigma_2/\sigma_1\sim e^{10}\sim10^4$. In such a case, Eq. (21) is clearly no longer valid in the energy range (E_1,E_2). In practice, the capture cross section should thus first be measured at different points in the density of states. In case σ is found to be a slowly varying function of energy, $N(E)$ can be obtained from a single spectrum for large-amplitude filling pulses using the axis transformation (20) and (21). In the opposite case, the density of states should be determined point by point, using appropriate energy windows as explained in the preceding sections.

E. Electric field effects on carrier emission

The electric field at the interface is a constitutive property of charged grain boundaries. Depending on the magnitude of the boundary charge (typically between 10^{11} and 10^{12} electrons per cm^2) and the applied voltage, the field can range from a few 10^3 up to some 10^5 V cm^{-1}. In such conditions, an effect of the electric field on carrier emission is not to be excluded. Transient capacitance measurements provide the means to investigate this possibility, as the emission rate from the boundary states can be measured under different field conditions. For this purpose, let us perform a set of DLTS recordings with a given filling-pulse amplitude (V_a) and different bias voltages (V_b); should the emission rate at the level E_{Fa} be field dependent, a shift of the inflection point (P_i) to lower temperatures would be expected for increasing values of V_b.

Figure 2 gives an example of a situation where field effects are negligible, as spectra (1) and (3) show no detectable shift of the inflection point for values of V_b between 0 and 4 V. On the other hand, field-enhanced emission has been apparently observed in the case of a low angle tilt boundary in germanium.[14] Signatures performed under different biasing conditions then showed a decrease of the activation energy of the boundary traps as a function of voltage V_b, of up to 0.1 eV for electron states located ~0.4 eV below the bottom of the conduction band. More experimental data will be needed, however, before definite conclusions can be drawn on this important subject.

IV. DISCUSSION OF AN EXAMPLE

A. Sample description and preparation

The results presented have been obtained for the $\Sigma=25$ twin boundary in a p-type doped silicon bicrystal. The geometrical parameters of the twin are as follows: boundary plane {710}; tilt axis ⟨001⟩; tilt angle 16.26°. The bicrystal is boron doped to 8.0×10^{14} cm^{-3}, corresponding to a room-temperature resistivity of 16.5 Ω cm. The boundary in as-grown specimens shows no electrical activity. On the other hand, barrier effects appear following appropriate heat treatments.[9] In the present case, the sample was annealed for 24 h at 900 °C under nitrogen flow. The specimen for the electrical measurements was cut in the shape of a parallelepiped $\sim3\times3\times10$ mm^3 with the grain boundary perpendicular to the longer dimension of the sample. Ohmic contacts were taken at both extremities and the specimen was then mounted in a variable-temperature cryostat equipped with shielded wires for capacitance measurements.

B. Preliminary thermally-stimulated-capacitance and capacitance-voltage measurements

As a preliminary step, low-temperature capacitance-voltage (C-V) and thermally-stimulated-capacitance (TSCAP) measurements were made in order to evaluate the total number of states at the interface. Additionally, these experiments also provide a useful check of the homogeneity of the dopant distribution within the space-charge region of the boundary.

In the TSCAP experiment,[18] excess carriers are stored at the interface levels by cooling the sample down to the liquid-nitrogen temperature under dc voltage V_0. At this point, let us remove the applied voltage and allow the sample to heat up gradually to room temperature; the boundary charge then relaxes towards equilibrium by thermal emission of the excess carriers. The emission process is readily detected by the concomitant variation

of the boundary capacitance. Figure 6(a) represents the variation of the capacitance as a function of temperature for different values of V_0 between 0 and 100 V: as is apparent from these curves, the release of the excess carriers occurs in an extended temperature range between ~ 100 and 260 K. A detailed discussion of these curves for different heating rates leads to an evaluation of the density of interface states, similar to that obtained by DLTS. However, our purpose in the present context is only to give evidence for the freezing of carrier emission at the liquid-nitrogen temperature.

Consider then the capacitance-voltage characteristics measured at 77 K [Fig. 6(b)]. Starting from zero bias, the voltage is gradually increased up to 50 V, the ramp rate being 0.2 V/s. As the voltage increases, the capacitance decreases due to a growing amount of carriers being trapped at the boundary levels [dotted line in Fig. 6(b)]. Due to the freezing of carrier emission, however, the boundary charge does not show a reversible variation as a function of voltage. (Similar charge memory effects were reported long ago on grain boundaries in germanium under light illumination at low temperatures.[19]) This charge memory effect is simply demonstrated by performing repeated voltage cycles between 0 V and some maximum voltage V_0: following its initial decrease on the first voltage run, the capacitance remains practically constant on further cycling, with a value uniquely dependent on the filling voltage V_0. This behavior is represented by the set of curves in solid line [Fig. 6(b)] for values of V_0 up to 50 V. [The boundary has identical properties for both polarities of the applied voltage, so that the cycles can be extended to the range $(V_0, -V_0)$.] Clearly each curve in this set corresponds to a fixed value of the boundary charge, uniquely determined by the filling voltage V_0.

The charge memory effect has an indirect application in checking the homogeneity of the doping level in the vicinity of the boundary.[20] For a fixed boundary charge, the C-V curve of the boundary is clearly only dependent on the dopant distribution in the vicinity of the interface. In the present case, it is concluded from the flatness of the C-V curves that the doping level is very nearly homogeneous within the space-charge region of the boundary, with a value equal to the doping level in the bulk $\sim 8.0\times 10^{14}$ cm^{-3}.

Consider last the C-V curve (dotted line) in Fig. 6(b): from this curve, the boundary charge can be evaluated as a function of the filling voltage using Eq. (3). The zero-bias boundary charge is $Q_0 = 1.4\times 10^{11}\ e\ \text{cm}^{-2}$. It increases to $Q_m = 1.02\times 10^{12}\ e\ \text{cm}^{-2}$ for $V_0 = 100$ V [using the TSCAP data of Fig. 6(a)]. These curves also indicate the amplitude of the voltage pulses to be used in DLTS measurements: pulses up to a hundred volts should be applied to measure all those states detected by the TSCAP and C-V experiments.

C. DLTS measurements

Figure 7(a) represents [curve (1)] the spectrum obtained for 100 V filling pulses, V_b being taken equal to 0 V. The pulse width and repetition times are 100 and 500 ms, respectively. t_1 and t_2 are taken equal to 88 and 338 ms, respectively, giving $t_2/t_1 = \frac{27}{7}$ and $g(E_{Fa})e_p(E_{Fa}) = 4$ s^{-1} (e_p denotes the hole emission rate in the case of p-type specimens). The spectrum shows a broad continuum with some modulation of the signal amplitude in the high-temperature range, and a sharp maximum (P) at

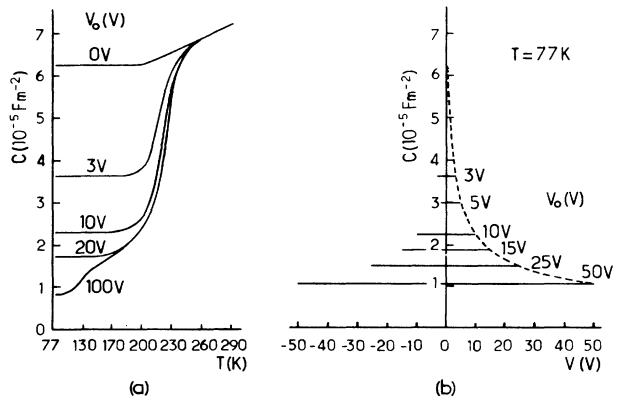

FIG. 6. (a) Thermally-stimulated-capacitance experiment on the $\Sigma = 25$ boundary levels in a p-type silicon bicrystal, boron doped to 8.0×10^{14} cm^{-3}. Sample annealed for 24 h at 900°C under nitrogen flow. Rate of temperature increase ~ 7°C/min. (b) Dotted line: capacitance-voltage curve of the boundary at 77 K. Ramp rate: 0.2 V/s. On repeated cycling, the capacitance takes a constant value uniquely determined by the filling voltage V_0. The set of solid curves represents the C-V curves obtained for different values of V_0 between 0 and 50 V.

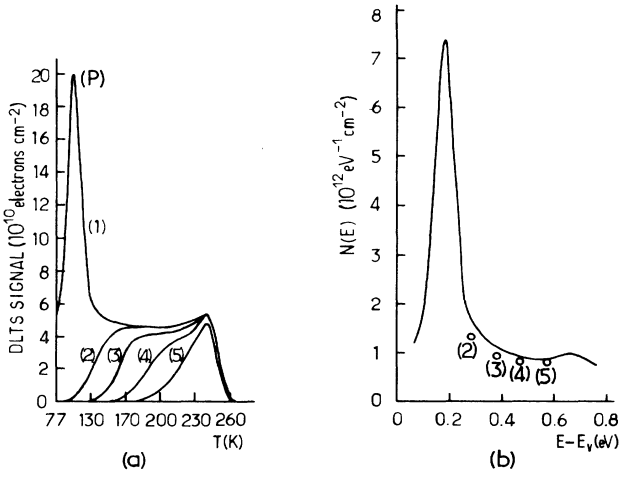

FIG. 7. (a) DLTS spectra for the same specimen as Fig. 6, with $g(E_{Fa})e_p(E_{Fa}) = 4$ s^{-1}. Spectrum (1): $V_a = 100$ V, $V_b = 0$ V. Spectrum (2): $V_a = 16$ V, $V_b = 0$ V. Spectrum (3): $V_a = 8$ V, $V_b = 0$ V. Spectrum (4): $V_a = 4$ V, $V_b = 0$ V. Spectrum (5): $V_a = 2$ V, $V_b = 0$ V. (P) denotes the low temperature peak on spectrum (1). (b) Solid line: density of states deduced from spectrum (1), using the axis transformation of Sec. III D. The open circles represent the density of states at the level E_{Fa} for spectra (2), (3), (4), and (5), respectively.

the low-temperature edge. Additional spectra were made using smaller pulse amplitudes: 16 V (2), 8 V (3), 4 V (4), and 2 V (5). The coordinates (T_i,S_i) of the inflection point on each of the spectra (2)–(5) were recorded in accordance with the procedure of Sec. III B.

Figure 8(a) represents, voltage by voltage, the signature of the traps at the quasi-Fermi level E_{Fa}. As the pulse amplitude increases, the QFL is shifted gradually from deep to shallower states. The shallowest level detected is associated with the peak (P). The signature of this trap gives an energy level 0.18 eV above the top of the valence band. Shallower states (if any) would require for their detection still higher voltages than were used for the present experiments.

Complementary current-voltage measurements were made to determine the capture cross sections of the traps as discussed in Sec. III C. In each case, $\sigma(E_{Fa})$ was determined for several temperatures where both $j(V_a)$ and $g(E_{Fa})e_p(E_{Fa})$ had been measured [Fig. 8(b)]. The capture cross sections are on the order of 10^{-14} to a few 10^{-13} cm^2. The error bars on these values are on the order of 50% due to variations of the current density on repeated measurements.

In order to obtain the density of states [Fig. 7(b)], the QFL's for different pulse amplitudes were first located along the energy axis in accordance with the signatures of Fig. 8(a). $N(E_{Fa})$ at these points was determined from the amplitude of the DLTS signal at the inflection points using Eq. (15) [open circles in Fig. 7(b)]. To complete these data, $N(E)$ was also deduced from the spectrum for 100 V pulses using Eq. (21). The density thus obtained (curve in solid line) fits within 20% with the values measured at the inflection points of the spectra.

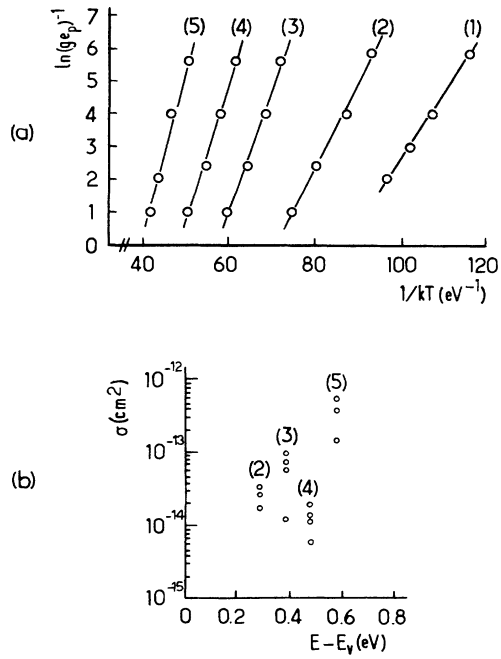

FIG. 8. (a) (1): Signature of the peak (P) on spectrum (1) [Fig. 7(a)], giving an energy level 0.18 eV above the top of the valence band. (2)–(5): Signatures of the QFL's for spectra (2)–(5), giving energy levels, respectively, at $E_v+0.28$ eV (spectrum 2), $E_v+0.38$ eV (spectrum 3), $E_v+0.47$ eV (spectrum 4), and $E_v+0.58$ eV (spectrum 5). ge_p represents the product of the trap degeneracy times the hole emission rate, expressed in s^{-1}. (b) The capture cross section at the level E_{Fa} for spectra (2), (3), (4), and (5), respectively. The circles refer to values of σ obtained for different temperatures where both $j(V_a)$ and $g(E_{Fa})e_p(E_{Fa})$ were determined.

The density of states takes values on the order of 10^{12} eV^{-1} cm^{-2} in the energy range 0.2–0.6 eV above the top of the valence band, with a sharp increase to $\sim 10^{13}$ eV^{-1} cm^{-2} at $E_v+0.18$ eV. The integrated amount of traps as obtained from the area under the curve $N(E)$ is $(9\pm2)\times10^{11}$ cm^{-2}, in good agreement with the value deduced from the C-V and TSCAP measurements (Sec. IV B): $Q_m-Q_0=8.8\times10^{11}\,e$ cm^{-2}. It is also of interest to estimate the amount of traps at the prominent level $E_v+0.18$ eV. For this purpose, we may evaluate the area under the peak (P) in the density of states; alternatively, we can also apply Eq. (5) relating the density of a single trap level to the peak amplitude of the DLTS signal. Both methods give values on the same order of magnitude: $\sim2\times10^{11}$ cm^{-2}.

V. CONCLUSION

A procedure has been developed for the quantitative evaluation of the DLTS spectra associated with a continuum of grain-boundary states. The method is based on a formal treatment of the associated nonexponential emission transients, leading to simple analytical expressions for the emission rate, the density of states, and the capture cross section at the quasi-Fermi level of the trapped carriers. With minor modifications, this treatment will also apply to different systems where interface states form a continuous distribution in energy, e.g., the states at oxide-semiconductor interfaces. Means to detect field-enhanced emission are also considered, as the electric field at the interface is apt to strongly influence the rate of carrier emission from the boundary states.

As a practical application, the grain-boundary parameters have been measured for the $\Sigma=25$ twin boundary in n- and p-type doped silicon bicrystals. In n-type silicon, a single boundary level is found at $E_c-0.66$ eV, with a density of 2.6×10^{11} cm^{-2}. In p-type silicon, the boundary levels are continuously distributed in energy, with a density on the order of 10^{12} eV^{-1} cm^{-2} in the energy range ($E_v+0.2$ eV, $E_v+0.6$ eV). The density of states shows a sharp maximum at $E_v+0.18$ eV, associated with a single trap level, the density of which is about 2×10^{11} cm^{-2}. The capture cross sections are on the order of 10^{-14} to a few 10^{-13} cm^2. These data are consistent with those obtained from complementary capacitance-voltage and thermally-stimulated-capacitance measurements.

The outstanding question behind these experiments is that of the nature of the boundary states. DLTS measurements on the $\Sigma=25$ boundary in silicon have shown a definite dependence of the electronic properties of the interface on the thermal history of the bicrystals.[9] The electrical activity of the boundary correlates with the

presence of impurity precipitates observed by transmission electron microscopy. EBIC (electron-beam-induced current) experiments have also shown the importance of the precipitates as recombination centers for injected minority carriers:[21] thus it might well be that the boundary states detected by DLTS are actually associated with the matrix-precipitate interfaces. It is hoped to cast some light on this problem by a microanalytical study of the precipitates in relation with the thermal history of the specimens.

ACKNOWLEDGMENTS

This work has been supported in part by Electricité de France under Contract No. 1B5520. I am very much indebted to F. Battistella and A. Rocher for help in the preparation of the specimens, and to C. Dahms, P. Haasen, G. Petermann, and W. Szkielko for stimulating discussions.

APPENDIX: THE DLTS SPECTRUM ASSOCIATED WITH A CONTINUUM OF GRAIN-BOUNDARY STATES

1. Expression of the DLTS signal

We shall investigate the form of the DLTS spectrum for a continuum of levels of density $N(E)$ in an n-type doped bicrystal (Fig. 9). We start with Eq. (9) for the charge transient

$$\Delta Q(t)=q\int_{E_v}^{E_c} N(E)[f(E-E_{Fa})-f(E-E_{Fb})] \times \exp[-e_n(E)t]dE \ , \tag{A1}$$

where E_{Fa} and E_{Fb} represent the quasi-Fermi-levels of the trapped electrons under the voltages V_a and V_b, respectively. $e_n(E)$ is the carrier emission rate at the level E in the density of states:

$$e_n(E)=e_{n0}(E)\exp[(E-E_c)/kT] \ , \tag{A2}$$

where the prefactor $e_{n0}(E)$ is given in terms of the capture cross section $\sigma(E)$ and the trap degeneracy $g(E)$ by

$$e_{n0}(E)=[\sigma(E)/g(E)]N_c v_{\rm th} \ . \tag{A3}$$

For a quantitative evaluation of the DLTS signal we shall approximate $N(E)$, $\sigma(E)$, and $g(E)$ by step functions as pictured by Figs. 9(a) and 9(b). Let us select the voltages V_a and V_b so that E_{Fa} and E_{Fb} both belong to the same plateau in the density of states. Let us then denote by $\bar{N}$, $\bar{\sigma}$, and $\bar{g}$ the respective averages of $N(E)$, $\sigma(E)$, and $g(E)$ in the energy range (E_{Fb},E_{Fa}). As explained in Sec. II B, the emission transient actually involves only those states between E_{Fa} and E_{Fb}. Thus there is no loss in generality in substituting $\bar{N}$ for $N(E)$, $\bar{\sigma}$ for $\sigma(E)$, and $\bar{g}$ for $g(E)$ in Eqs. (A1) and (A3). $\Delta Q(t)$ then has the simplified expression

$$\Delta Q(t)=q\bar{N}\int_{E_v}^{E_c}[f(E-E_{fa})-f(E-E_{Fb})] \times \exp[-te_n(E)]dE \ . \tag{A4}$$

As a further simplification, we shall take e_{n0} to be constant as a function of temperature. This approximation is justified by the weak dependence of e_{n0} on T (in T^2) as compared with that of $e_n(E)$ in $\exp[(E-E_c)/kT]$ [Eq. (A2)]. With the variable change

$$u=\exp[(E-E_{Fa})/kT] \tag{A5}$$

the emission transient takes the form

$$\Delta Q(t)=q\bar{N}kT\int_{u_v}^{u_c}\left[\frac{1}{\theta\bar{g}+u}-\frac{1}{\bar{g}+u}\right] \times \exp[-ute_n(E_{Fa})]du \ , \tag{A6}$$

where

$$\theta=\exp[-(E_{Fa}-E_{Fb})/kT] \ , \tag{A7}$$

$$u_v=\exp[-(E_{Fa}-E_v)/kT] \ , \tag{A8}$$

and

$$u_c=\exp[-(E_{Fa}-E_c)/kT] \ . \tag{A9}$$

The DLTS signal is given by $S(t_1,t_2)=\Delta Q(t_1)-\Delta Q(t_2)$, which we rewrite in the form $S(t_1,t_2)=S_1(t_1,t_2)-S_2(t_1,t_2)$, where S_1 and S_2 are defined as follows:

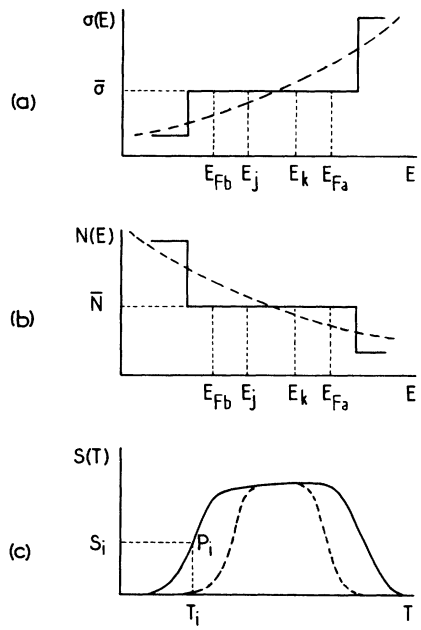

FIG. 9. (a) and (b) The capture cross section $\sigma(E)$ and the density of states $N(E)$ as a function of energy (dotted lines), and their schematic representation by step functions (solid lines). $\bar{\sigma}$ and $\bar{N}$ represent the respective averages of $\sigma(E)$ and $N(E)$ over the range (E_{Fb},E_{Fa}). E_j and E_k are any two levels with $E_{Fb}<E_j<E_k<E_{Fa}$. (c) The spectrum associated with the traps in the energy range (E_{Fb},E_{Fa}) (solid line), showing the inflection point $P_i(T_i,S_i)$. Dotted line: the contribution S_{jk} to the spectrum of the traps in the energy range (E_j,E_k).

$$S_1(t_1,t_2)=q\bar{N}kT\int_{u_v}^{u_c}\frac{\exp[-ut_1e_n(E_{Fa})]-\exp[-ut_2e_n(E_{Fa})]}{\theta\bar{g}+u}du \tag{A10}$$

and

$$S_2(t_1,t_2)=q\bar{N}kT\int_{u_v}^{u_c}\frac{\exp[-ut_1e_n(E_{Fa})]-\exp[-ut_2e_n(E_{Fa})]}{\bar{g}+u}du\ . \tag{A11}$$

Consider the upper (u_c) and lower (u_v) bounds of these integrals: under usual temperature and voltage conditions, E_{Fa} is separated by several kT at least from the valence- and the conduction-band edges so that $u_v \ll 1$ and $u_c \gg 1$. On account of these inequalities, the upper and lower bounds of S_1 and S_2 can be replaced by ∞ and 0, respectively. S_1 and S_2 then reduce to a combination of integrals of the form

$$\int_0^\infty \frac{\exp(-ax)}{x+b}dx\ .$$

Using the properties of the exponential integral,[13] we then obtain for S_1 and S_2 the following expressions:

$$S_1=q\bar{N}kT\ln(t_2/t_1) \tag{A12}$$

and

$$S_2(t_1,t_2)=q\bar{N}kT\{\exp[\bar{g}t_1e_n(E_{Fa})]\mathbb{E}_1(\bar{g}t_1e_n(E_{Fa}))-\exp[\bar{g}t_2e_n(E_{Fa})]\times\mathbb{E}_1(\bar{g}t_2e_n(E_{Fa}))\}\ , \tag{A13}$$

where $\mathbb{E}_1(x)$ is defined by Eq. (14) in the text. The DLTS signal is given by

$$S(t_1,t_2)=q\bar{N}kT\{\ln(t_2/t_1)+\exp[\bar{g}t_2e_n(E_{Fa})]\times\mathbb{E}_1(\bar{g}t_2e_n(E_{Fa}))-\exp[\bar{g}t_1e_n(E_{Fa})]\times\mathbb{E}_1(\bar{g}t_1e_n(E_{Fa}))\}\ . \tag{A14}$$

The variation of S as a function of temperature is represented by the solid curve in Fig. 9(c). The signal is zero at low T where $[\bar{g}e_n(E_{Fa})]^{-1}>t_2$. It then increases to a broad maximum at temperatures where $[\bar{g}e_n(E_{Fa})]^{-1}<(t_1,t_2)<[\bar{g}e_n(E_{Fb})]^{-1}$. All through that range, $S(T)$ has the simple approximate expression:

$$S\approx q\bar{N}kT\ln(t_2/t_1) \tag{A15}$$

with a linear dependence on temperature. S finally returns to zero at high temperatures where $[\bar{g}e_n(E_{Fb})]^{-1}<t_1$.

2. Determination of the emission rate and the density of states at the quasi-Fermi-level E_{Fa}

The inflection point $P_i(T_i,S_i)$ on the low-temperature edge of the spectrum is of particular interest in view of the fact that it can be easily recognized in practical cases. A straightforward calculation leads to

$$\frac{d^2S}{dT^2}=\frac{kuq\bar{N}}{T}\left[\frac{E_c-E_{Fa}}{kT}\right]^2\{r[(1+ru)e^{ru}\mathbb{E}_1(ru)-1]-[(1+u)e^{u}\mathbb{E}_1(u)-1]\}\ , \tag{A16}$$

where $r=t_2/t_1$ and $u=[\bar{g}t_1e_n(E_{Fa})]$. The temperature T_i is determined by the condition $d^2S/dT^2=0$. Referring to Eq. (A16), we then obtain the set of equations (11)–(14) in the text, giving the product $g(E_{Fa})e_n(E_{Fa})$ at $T=T_i$ as a function of the gate settings t_1 and t_2. On account of Eq. (A14), S_i then gives a measure of the density of states $N(E_{Fa})$ once $g(E_{Fa})e_n(E_{Fa})$ has been determined.

3. The energy resolution of DLTS measurements

The emission transient at T_i actually involves the boundary states in some energy range of width ΔE about E_{Fa}. ΔE represents the energy resolution of the DLTS measurement. To estimate ΔE, let us consider the contribution S_{jk} to the DLTS signal, of the traps in the range (E_j,E_k) with $E_{Fb}<E_j<E_k<E_{Fa}$ [Figs. 9(a) and 9(b)]. A calculation similar to that detailed for $S(t_1,t_2)$ gives

$$S_{jk}(t_1,t_2)=q\bar{N}kT[\mathbb{E}_1(\bar{g}t_2e_n(E_k))-\mathbb{E}_1(\bar{g}t_1e_n(E_k))+\mathbb{E}_1(\bar{g}t_1e_n(E_j))-\mathbb{E}_1(\bar{g}t_2e_n(E_j))]\ , \tag{A17}$$

where $e_n(E_j)$ and $e_n(E_k)$ are the emission rates at the levels E_j and E_k, respectively. The variation of S_{jk} with temperature is represented by the dotted line in Fig. 9(c): starting from zero at low T, S_{jk} comes in coincidence with $S(T)$ in the temperature range where $[\bar{g}e_n(E_k)]^{-1}<(t_1,t_2)<[\bar{g}e_n(E_j)]^{-1}$, then returns to zero at high temperatures. Consider in particular the value of S_{jk} at the temperature T_i: then, $\bar{g}t_2e_n(E_k)$ and the similar quantities on the right-hand side of Eq. (A17) are small compared with unity, so that S_{jk} has the expression

$$S_{jk}=q\bar{N}kT_i[\bar{g}(t_2-t_1)e_n(E_{Fa})]\times\{\exp[-(E_{Fa}-E_k)/kT_i]-\exp[-(E_{Fa}-E_j)/kT_i]\}\ . \tag{A18}$$

For $T=T_i$ the factor $[\bar{g}(t_2-t_1)e_n(E_{Fa})]$ is on the order of unity. Equations (A14) and (A18) then show S_{jk} will

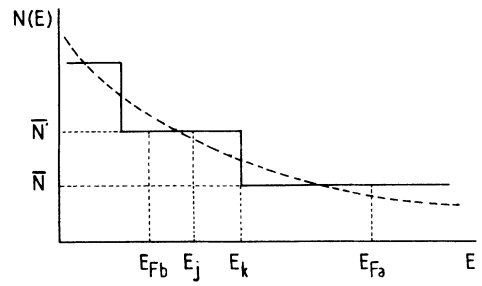

FIG. 10. Schematic representation of the density of states $N(E)$ with the quasi-Fermi-levels E_{Fa} and E_{Fb} located on two different plateaus (densities $\bar{N}$ and $\bar{N}'$). E_k represents the energy level where $N(E)$ changes from $\bar{N}$ to $\bar{N}'$.

be negligible compared with S_i, unless E_{Fa} and E_k differ by less than a few kT_i. Thus only those states in a range of energy ΔE comparable with the width of the quasi-Fermi-distribution $f(E-E_{Fa})$ have a significant contribution to the DLTS signal at T_i.

The value just given for ΔE represents the basic resolution of the DLTS measurement, obtained on the condition that the density of states has little variation in the energy range (E_{Fa},E_{Fb}). To estimate the effect on ΔE of large variations in the density of states, let us assume now E_{Fa} and E_{Fb} belong to two contiguous plateaus with the respective densities $\bar{N}$ and $\bar{N}'$, and take E_k to be the energy level where the density changes from $\bar{N}$ to $\bar{N}'$ (Fig. 10). Consider again the boundary levels between E_j and E_k: by a calculation similar to that of Eq. (A18), the contribution of those states to the DLTS signal at T_i is found to be

$$S'_{jk} \sim q\bar{N}'kT_i\{\exp[-(E_{Fa}-E_k)/kT_i] - \exp[-(E_{Fa}-E_j)/kT_i]\} . \quad \text{(A19)}$$

According to Eqs. (A14) and (A19), the condition that S'_{jk} should be small compared with S_i is

$$N(E_k) \ll N(E_{Fa})\exp[(E_{Fa}-E_k)/kT_i] . \quad \text{(A20)}$$

For a numerical estimate, let us take $E_{Fa}-E_k=0.1$ eV and $T_i=116$ K. The inequality (A20) then gives $N(E_k)/N(E_{Fa}) \ll e^{10} \sim 10^4$. Thus the energy resolution will be largely insensitive to variations of the density of states with energy, with an exception for the case where $N(E)$ varies by orders of magnitude in the vicinity of E_{Fa}.

[1]For a recent review, see C. R. M. Grovenor, J. Phys. C **18**, 4079 (1985).
[2]R. E. Thomson and D. J. Chadi, Phys. Rev. B **29**, 889 (1984).
[3]E. H. Nicollian and A. Goetzberger, Bell Syst. Tech. J. **46**, 1055 (1967).
[4]G. E. Pike, Phys. Rev. B **30**, 795 (1984).
[5]L. D. Yau and C. T. Sah, Phys. Status Solidi A **6**, 561 (1971).
[6]D. V. Lang, J. Appl. Phys. **45**, 3023 (1974).
[7]M. Spencer, R. Stall, L. F. Eastman, and C. E. C. Wood, J. Appl. Phys. **50**, 8006 (1979).
[8]A. Broniatowski, in *Polycrystalline Semiconductors, Physical Properties and Applications,* edited by G. Harbeke (Springer, Berlin, 1985), p. 95.
[9]A. Broniatowski, Rev. Phys. Appl. (Paris) **22**, 585 (1987).
[10]R. Stratton, Proc. Phys. Soc. London, Sect. B **69**, 513 (1956).
[11]The silicon bicrystals were provided by Cristaltec (Centre d'Etudes Nucléaires de Grenoble, France).
[12]K. Yamasaki, M. Yoshida, and T. Sugano, Jpn. J. Appl. Phys. **18**, 113 (1979).
[13]See, for instance, *Handbook of Mathematical Functions,* edited by A. Abramowitz and I. A. Stegun (Dover, New York, 1965), p. 228.
[14]A. Broniatowski, J. Phys. (Paris) **44**, C4-339 (1983).
[15]M. G. Spencer, W. J. Schaff, and D. K. Wagner, J. Appl. Phys. **54**, 1429 (1983).
[16]N. I. Bochkareva, Yu. S. Lelikov, M. D. Lyubalin, and Yu. G. Shreter, Fiz. Tekh. Poluprovodn. **20**, 1396 (1986) [Sov. Phys.—Semicond. **20**, 878 (1986)].
[17]P. C. Srivastava, J. C. Bourgoin, F. Rebajo, and J. M. Mimila Arroyo, J. Appl. Phys. **53**, 8633 (1982).
[18]C. T. Sah, W. W. Chan, H. S. Fu, and J. M. Walker, Appl. Phys. Lett. **20**, 193 (1972).
[19]R. K. Mueller, J. Appl. Phys. **30**, 1004 (1959).
[20]A. Broniatowski (unpublished).
[21]F. Battistella, A. Rocher, and A. George, Proc. Mater. Res. Soc. **59**, 347 (1986).